

Slepton mass splittings and cLFV in the SUSY seesaw in the light of recent experimental results

A. J. R. Figueiredo^{a,b} and A. M. Teixeira^b

^a Centro de Física Teórica de Partículas, Instituto Superior Técnico,
Av. Rovisco Pais 1, 1049-001 Lisboa, Portugal

^b Laboratoire de Physique Corpusculaire, CNRS/IN2P3 – UMR 6533,
Campus des Cézeaux, 24 Av. des Landais, F-63177 Aubièrre Cedex, France

Abstract

Following recent experimental developments, in this study we re-evaluate if the interplay of high- and low-energy lepton flavour violating observables remains a viable probe to test the high-scale type-I supersymmetric seesaw. Our analysis shows that fully constrained supersymmetric scenarios no longer allow to explore this interplay, since recent LHC data precludes the possibility of having sizeable slepton mass differences for a slepton spectrum sufficiently light to be produced, and in association to $\text{BR}(\mu \rightarrow e\gamma)$ within experimental reach. However, relaxing the strict universality of supersymmetric soft-breaking terms and fully exploring heavy neutrino dynamics, still allows to have slepton mass splittings $\mathcal{O}(\text{few } \%)$, for slepton masses accessible at the LHC, with associated $\mu \rightarrow e\gamma$ rates within future sensitivity. For these scenarios, we illustrate how the correlation between high- and low-energy lepton flavour violating observables allows to probe the high-scale supersymmetric seesaw.

1 Introduction

Supersymmetric (SUSY) seesaw realisations offer an appealing framework to address several of the observational and theoretical shortcomings of the Standard Model (SM). Even if realised at a very high-scale (close to the grand unification scale, M_{GUT}), prior to their decoupling, the new right-handed neutrino superfields induce corrections into the SUSY soft-breaking slepton terms. Since neutrino oscillations do not conserve lepton flavour, these corrections are lepton flavour violating (LFV), and can induce SUSY contributions to slepton mediated charged LFV (cLFV) observables [1].

Compared to its non-SUSY version [2], and in addition to accounting for neutrino masses and mixings, the high-scale type-I SUSY seesaw opens the door to a large number of cLFV observables at/below the TeV scale, that can be searched for in low-energy, high intensity facilities or in high-energy colliders as the LHC or a future Linear Collider (LC). Among the former one has flavour violating radiative and three body lepton decays, as well as muon-electron conversion in nuclei [3–26]; the latter are associated to the potential reconstruction of SUSY decay chains involving slepton intermediate states, and include various observables, such as for example flavoured slepton mass differences and direct flavour violating gaugino decays [27–41].

However, in the absence of SUSY discovery (and reconstruction of its fundamental Lagrangian), the contributions to the different cLFV observables allow for a wide range of predictions, as the

observables are in general dependent on powers of the average SUSY scale and of the seesaw scale. While the first might be possibly known in the near future, the second cannot be directly probed, which renders these scenarios hard to test. However, when embedded into flavour blind SUSY breaking models, the type-I seesaw is the unique source of flavour violation in the lepton sector, implying that all lepton flavour violating observables will be correlated. The study of the synergy between different low-energy observables and/or high-energy ones proves to be a powerful tool to probe the high-scale type-I SUSY seesaw (see, for example, [30, 32, 33, 35, 37, 40]).

Since the first related analyses, important experimental developments have occurred, in a number of fronts. Firstly, θ_{13} has been measured [42–45], its value being sizeable. Regarding high-energy experiments, LHC negative searches on SUSY particles suggest a considerably heavier SUSY spectrum [46–51], which puts increasingly stronger bounds on the parameter space of constrained SUSY models. Accommodating the measured mass of the recently discovered SM-like Higgs boson [52] renders the latter bounds even more severe. Finally, the MEG experiment has significantly improved the upper bounds on $\text{BR}(\mu \rightarrow e\gamma)$ [53]. In view of the latter developments, it is important to re-evaluate the prospects of probing the type-I SUSY seesaw via the synergy between slepton mass differences (if measured at the LHC) and low-energy cLFV observables such as $\text{BR}(\mu \rightarrow e\gamma)$. Charged sleptons may indeed be discovered in the forthcoming $\sqrt{s} = 14$ TeV LHC run or then in the subsequent high luminosity phase, for which an integrated luminosity ~ 3000 fb $^{-1}$ is expected [54, 55]. If indeed discovered, promising windows over the lepton flavour puzzle can be opened, with prospects for shedding light on the mechanism of neutrino mass generation¹.

The aim of the present study is thus to discuss whether sleptons with inter-generational mass differences (resulting mainly from a high-scale type-I SUSY seesaw), compatible with current cLFV results and negative SUSY searches, can be seen in future LHC runs, and how such observations would in turn affect the information one could derive on the seesaw parameters. To do so, we consider the embedding of a type-I seesaw into constrained SUSY models, in particular into the constrained minimal supersymmetric standard model (cMSSM), extended by three generations of right-handed neutrino superfields. We then relax some of the cMSSM strict universality conditions for the different sectors, still preserving flavour universality. We discuss the impact of these scenarios on high-energy cLFV observables as slepton mass differences (between sleptons of different families), while at low-energies we focus on $\mu \rightarrow e\gamma$ decays and $\mu - e$ conversion in Nuclei.

The paper is organised as follows. In Section 2 we briefly describe the type-I SUSY seesaw model and its most relevant phenomenological signatures. In Section 3 we present the analysis and discuss the results; our conclusions are summarised in Section 4.

2 The SUSY seesaw model

The type-I SUSY seesaw consists of the Minimal Supersymmetric Standard Model (MSSM), extended by three generations of right-handed neutrino (chiral) superfields $\hat{N}_i^c \sim (\nu^c, \tilde{\nu}_R^*)_i$. The leptonic part of the superpotential reads

$$\mathcal{W}^{\text{lepton}} = \hat{N}^c Y^\nu \hat{L} \hat{H}_2 + \hat{E}^c Y^l \hat{L} \hat{H}_1 + \frac{1}{2} \hat{N}^c M_R \hat{N}^c, \quad (1)$$

where \hat{L} and \hat{E}^c denote the SU(2) lepton doublet and right-handed charged lepton superfields, respectively, and $\hat{H}_{1,2}$ are the two Higgs supermultiplets. Without loss of generality, we work in

¹A recent work has revisited charged cLFV signatures, within a SU(5) GUT framework, in low-energy observables and in flavour violating neutralino decays [41]. Low-energy cLFV in the framework of an SO(10) embedded type-I SUSY seesaw, taking into account the constraints from m_h , was discussed in [56].

a basis where both the charged lepton Yukawa couplings Y^l and the Majorana mass matrix M_R are diagonal. For completeness², the slepton soft breaking potential is given by

$$\begin{aligned} \mathcal{V}_{\text{soft}}^{\text{slepton}} &= \tilde{\ell}_L^* m_L^2 \tilde{\ell}_L + \tilde{\ell}_R^* m_E^2 \tilde{\ell}_R + \tilde{\nu}_R^* m_{\tilde{\nu}_R}^2 \tilde{\nu}_R \\ &+ \left(\tilde{\ell}_R^* A^l \tilde{\ell}_L H_1 + \tilde{\nu}_R^* A^\nu \tilde{\nu}_L H_2 + \frac{1}{2} \tilde{\nu}_R B_\nu \tilde{\nu}_R + \text{H.c.} \right). \end{aligned} \quad (2)$$

We consider a flavour-blind SUSY breaking mechanism (so that the Yukawa couplings are the only source of flavour violation), as for example the case of minimal supergravity mediated SUSY breaking, assuming that the soft breaking parameters satisfy universality conditions at some high-energy scale, which we take to be the gauge coupling unification scale, $M_{\text{GUT}} \sim 10^{16}$ GeV:

$$M_i^\psi = M_{1/2}, \quad (m_\phi^2)_{ij} = \delta_{ij} m_0^2, \quad (A_\phi)_{ij} = A_0^\phi (Y^\phi)_{ij}. \quad (3)$$

In the seesaw limit (i.e., $Y^\nu v_2 \ll M_R$), after electroweak (EW) symmetry breaking, the light neutrino mass matrix is approximately given by $m_\nu \simeq -v_2^2 Y^{\nu T} M_R^{-1} Y^\nu$, where v_2 is one of the vacuum expectation values of the neutral Higgs H_i ($v_{1(2)} = v \cos(\sin)\beta$, with $v = 174$ GeV). As suggested from the seesaw expression for m_ν , a convenient means of parameterising the neutrino Yukawa couplings Y^ν , while at the same time allowing to accommodate neutrino data, is given by the Casas-Ibarra parameterisation [10]. At the seesaw scale one can write

$$Y^\nu = \frac{i}{v_2} \sqrt{M_R^{\text{diag}}} R \sqrt{m_\nu^{\text{diag}}} U^{\text{MNS}\dagger}, \quad (4)$$

which we will use in our numerical analysis. In the above, U^{MNS} is the leptonic mixing matrix and R is a complex orthogonal matrix, parameterised in terms of three complex angles (θ_i), that encodes additional mixings involving the right-handed (RH) neutrinos; m_ν^{diag} and M_R^{diag} respectively denote the (diagonal) light and heavy neutrino mass matrices.

2.1 Flavour violation in the slepton sector

Due to the non-trivial flavour structure of Y^ν , the running from M_{GUT} down to the seesaw scale M_R will induce flavour mixing in the otherwise (approximately) flavour conserving slepton soft breaking terms [1]. This running is more pronounced in the “left-handed” soft breaking terms (i.e., the terms involving slepton doublets). At leading order (leading logarithm (LLog) approximation), the flavour mixing induced by the renormalisation group (RG) flow reads

$$\left(\Delta m_L^2 \right)_{ij} = -\frac{1}{8\pi^2} \left(m_L^2 + m_{\tilde{\nu}_R}^2 + m_{H_2}^2 + |A_0^\nu|^2 \right) \left(Y^{\nu\dagger} L Y^\nu \right)_{ij}, \quad (5)$$

$$\left(\Delta A^l \right)_{ij} = -\frac{1}{16\pi^2} \left(A_0^l + 2A_0^\nu \right) Y_{ii}^l \left(Y^{\nu\dagger} L Y^\nu \right)_{ij}; \quad L_{kl} \equiv \log \left(\frac{M_{\text{GUT}}}{M_{R_k}} \right) \delta_{kl}. \quad (6)$$

As is clear from the above, the amount of flavour violation in the slepton sector is encoded in $\left(Y^{\nu\dagger} L Y^\nu \right)_{ij}$, originating from light neutrino mixing and from possible mixings involving the heavy neutrinos (see Eq. (4)). Having a unique source of LFV is the key to all tests of the SUSY seesaw; this becomes particularly clear in the simple (conservative) limit in which one assumes little (or

²Since we work in a regime $M_R \gg m_{\text{soft}}$ the effects of the B_ν -term (assumed to be $B_\nu \sim m_{\text{soft}}^2$) become negligible in comparison to the superpotential mass term ($\tilde{\nu}_R^* M_R^2 \tilde{\nu}_R$) – see for e.g. [57] for a discussion –, and will not be taken into account in the analysis.

no) additional mixing involving the heavy RH states (i.e., $R \sim \mathbb{1}$). To a good approximation, the intrinsic amount of cLFV is related to low-energy leptonic mixings as

$$\left(Y^{\nu\dagger} L Y^\nu \right)_{ij} \simeq U_{ik}^{\text{MNS}} U_{jk}^{\text{MNS}*} (m_k M_{R_k} L_k). \quad (7)$$

Considering ratios of cLFV observables with similar loop dynamics - approximately equal to ratios of the above quantity -, firstly allows to test the SUSY seesaw by checking whether or not its degrees of freedom can accommodate the value of (future) measured quantities. In turn, this may then allow to extract information on the heavy spectrum, M_{R_k} (although there is still a dependence on the neutrino mass hierarchy and U^{MNS} phases). On the other hand, by comparing observables with different loop dynamics but similar flavour structure (e.g., $\ell_i \rightarrow 3\ell_j$ and $\ell_i \rightarrow \ell_j\gamma$) one may test new sectors where LFV can be present.

2.2 Slepton induced cLFV observables

Slepton flavour mixing can lead to charged lepton flavour violation, manifest in a wide array of observables, at both low-energies (rare processes searched for at high-intensity experiments, such as MEG and BaBar) and high energies (at colliders, above the slepton production threshold). Having one unique source of flavour violation implies that the observables should exhibit some correlation which, as extensively discussed in the literature (see, for example, [30,32,33,35,37,40]), allows to indirectly probe the high-scale seesaw hypothesis.

At low-energies, virtual sleptons can mediate flavour violating lepton transitions, such as radiative decays, three-body decays and conversion in nuclei. As an example, the radiative decay $\ell_i \rightarrow \ell_j\gamma$ receives contributions originating from sneutrino-chargino and charged slepton-neutralino loops (see e.g. [58], and references therein). Compared to the SM contributions, which are highly suppressed by powers of m_ν/M_W , these new contributions can be sizeable provided $m_{\tilde{\ell}_L}$ is not *too heavy* and slepton flavour mixing is large. An analytical understanding of the dependency of $\text{BR}(\ell_i \rightarrow \ell_j\gamma)$ on the neutrino Yukawa couplings can be obtained using the LLog approximation. In the limit of very small off-diagonal $\Delta m_{\tilde{L}}^2$ entries, one has

$$\frac{\text{BR}(\ell_i \rightarrow \ell_j\gamma)}{\text{BR}(\ell_i \rightarrow \ell_j\nu_i\bar{\nu}_j)} \approx \frac{\alpha^3 \tan^2 \beta}{G_F^2 m_{\text{SUSY}}^8} \left| \frac{1}{8\pi^2} \left(m_{\tilde{L}}^2 + m_{\tilde{\nu}_R}^2 + m_{H_2}^2 + |A_0^\nu|^2 \right) \left(Y^{\nu\dagger} L Y^\nu \right)_{ij} \right|^2. \quad (8)$$

The current experimental sensitivity to slepton flavour mixing, i.e. to $(\Delta m_{\tilde{L}}^2)_{ij}$, in other observables such as $\ell_i \rightarrow \ell_j\bar{\ell}_k\ell_k$ and $\text{CR}(\mu - e, \text{N})$, is in general smaller than in $\ell_i \rightarrow \ell_j\gamma$ [59]. The current 90% C.L. upper-limits on the cLFV radiative decays are [53,60]

$$\text{BR}(\mu \rightarrow e\gamma) < 5.7 \times 10^{-13}, \quad \text{BR}(\tau \rightarrow \mu\gamma) < 4.4 \times 10^{-8}, \quad \text{BR}(\tau \rightarrow e\gamma) < 3.3 \times 10^{-8}. \quad (9)$$

Under the assumption that all off-diagonal entries $(Y^{\nu\dagger} L Y^\nu)_{ij}$ are of the same order of magnitude, the limit on $\text{BR}(\mu \rightarrow e\gamma)$ turns out to be the most constraining. In view of this, and given the very recent experimental MEG bound on the $\text{BR}(\mu \rightarrow e\gamma)$ [53], in the present update we mainly focus on the constraints arising from $\mu \rightarrow e\gamma$.

At high-energy colliders, slepton flavour mixing can be directly probed through $\tilde{\ell}_{Li} \rightarrow \ell_j\chi_1^0$ decays [28,31,33,35,36,40,41]. At the LHC sleptons are preferably produced in cascade decays of the form $\tilde{q}_L \rightarrow \{\chi_2^0, \chi_1^\pm\}q' \rightarrow \tilde{\ell}_L\{\ell, \nu\}q'$, provided that these are kinematically allowed. Alternatively, sleptons can also be present in the decay chains of directly produced wino-like χ^0 and χ^\pm , which then decay to $\tilde{\ell}_L$. If both these modes are not viable, then direct production of slepton pairs

through Drell-Yann s-channel γ and Z exchanges becomes the only possible slepton production mode³.

Despite the missing energy signature which is always present in R-parity conserving SUSY models with a neutral lightest SUSY particle (LSP), strategies to reconstruct sparticle masses have been devised [61–63]. These rely on the assumption that sparticles typically decay to ordinary particles through two body cascade decays, and that the invariant masses that can be formed by combining the momenta of the so-produced SM particles give rise to structures with edges (whose end-points are simple functions of sparticle masses). Assuming that the wino-like χ_2^0 is heavier than the sleptons, the edge structure of the di-lepton invariant mass distributions ($m_{\ell\ell}$) is sensitive to slepton masses due to the decay $\chi_2^0 \rightarrow \tilde{\ell}\ell \rightarrow \ell\ell\chi_1^0$. An interesting effect of a high-scale SUSY seesaw is the appearance of a third edge in the di-lepton invariant mass distribution, due to an intermediate slepton of a different flavour (i.e., $\tilde{\ell}_j \rightarrow \ell_i\chi_1^0$), a consequence of slepton flavour mixing (see the detailed analysis of [35]).

2.3 Flavoured slepton mass differences

Here we focus on the mass differences between sleptons of different generations (especially the first two, which are dominated by either the left- or right-handed slepton component). In the absence of LFV, flavoured or inter-generational slepton mass differences arise from both Y^l and in A^l (with $A^l = A_0^l Y^l$ at the GUT scale); due to the smallness of the electron and muon Yukawa couplings ($Y_{(11,22)}^l$), the mass differences between the first two generations is in general well below the $\mathcal{O}(0.1\%)$ level [35], even in the case of large $\tan\beta$.

Through RG-induced effects involving Y^ν (see the previous subsections), the seesaw introduces additional contributions to slepton mass differences. As is clear from Eq. (5), these appear in the form of flavour diagonal and non-diagonal contributions to the slepton soft masses. Moreover, and even in the absence of flavour-violating effects (i.e., $i = j$), their effects are manifest in an enhancement of the fractional splittings between $m_{\tilde{e}_L}$ and $m_{\tilde{\mu}_L}$ (no significant effect in the right-handed slepton sector, as LFV in the SUSY seesaw is mostly a left-handed phenomenon), which are defined as

$$\frac{\Delta m_{\tilde{\ell}}}{m_{\tilde{\ell}}}(\tilde{e}_L, \tilde{\mu}_L) = \frac{|m_{\tilde{e}_L} - m_{\tilde{\mu}_L}|}{\langle m_{\tilde{e}_L}, m_{\tilde{\mu}_L} \rangle}. \quad (10)$$

Although in the presence of non-negligible flavour violation the slepton eigenstates correspond to a mixture of the three flavours, we will assume here that the states identified by $\tilde{\ell}_L$ are dominated by the corresponding flavour component.

Previous studies [35] (before recent 2013 LHC and MEG results) had suggested that splittings as large as $\sim 10\%$ could indeed be obtained for sleptons lighter than 1 TeV. As mentioned before, we now proceed to re-evaluate these claims, in view of recent MEG bounds and LHC search results.

3 Numerical results and discussion

In our numerical analysis we assume a normal hierarchy for the light neutrino spectrum, with non-vanishing m_{ν_1} (which we set $\approx \mathcal{O}(10^{-5} \text{ eV})$). The squared neutrino mass differences, as well as the neutrino mixing angles (for a standard parameterisation of the U^{MNS}), are taken in the intervals favoured by current best fits [64]. In our analysis we will assume vanishing CP phases (Dirac and Majorana).

³For a discussion of the prospects of LFV in slepton decays at a future Linear Collider see, for example, [40].

We compute the SUSY spectrum and couplings using the public code SPHENO-3.2.2 [65], extended by additional routines to fit the high-scale neutrino Yukawa couplings as to yield the observed oscillation data. We require that the lightest Higgs state, h , be compatible with recent LHC data on a SM-like scalar boson [52]. In addition to having m_h in the range [123 GeV, 128 GeV], we further require that its couplings are not excluded at 95% C.L. by current data using HIGGSBOUNDS-4.0.0 [66]. Concerning the sparticle spectrum, we have imposed the following (conservative) bounds: all LEP bounds [67] were enforced; the gluino and first two generation squarks are required to be heavier than the upper-limits of [46] (derived in the limit of $m_{\chi_1^0} = 0$); bounds on the 3rd generation squark masses [47], $m_{\chi_2^0}$, $m_{\chi_1^\pm}$ [48, 49] and $m_{\tilde{\ell}}$ [50] are also imposed (again in simplified models with $m_{\chi_1^0} = 0$). If the LSP is charged (solutions which are disfavoured in our phenomenological analysis), we nevertheless require its mass to be above the most constraining lower-limit derived from searches for heavy stable charged particles at the LHC [51]. Finally, the dark-matter relic density is calculated with MICROMEGAS-3.0.24 [68].

In our analysis we first begin by considering minimal supergravity (mSUGRA) inspired universality conditions, and afterwards study the impact of relaxing these universality conditions. This serves different purposes. First, to identify the regions of the parameter space offering the most promising prospects for observation of slepton mass differences at forthcoming LHC runs which, besides providing a SM-like Higgs, are compatible with the most recent low energy cLFV and sparticle bounds. Secondly, our aim is to investigate whether the synergy of such mass differences (measurements or upper bounds) and the future results on low energy cLFV could still suggest some hints on the heavy neutrino spectrum (now rendered easier as all light neutrino mixing angles have been measured).

3.1 mSUGRA-inspired universality

We first consider an mSUGRA inspired framework, requiring that at M_{GUT} the SUSY soft-breaking parameters are universal as in cMSSM, and imposing the following relations on the additional seesaw soft-breaking terms:

$$(m_{\nu_R}^2)_{ij} = \delta_{ij}m_0^2, \quad (A^\nu)_{ij} = A_0(Y^\nu)_{ij}, \quad (11)$$

where m_0 and A_0 are the universal scalar soft-breaking mass and trilinear couplings of the cMSSM. We begin our analysis by revisiting the m_0 - $M_{1/2}$ plane, and evaluate the joint impact of the recent MEG bound on $\text{BR}(\mu \rightarrow e\gamma)$ and of the LHC negative SUSY searches. This further allows to determine the experimentally viable regions offering the best prospects concerning the study of slepton mass splittings.

In Fig. 1 we present the m_0 - $M_{1/2}$ plane⁴ for different choices of A_0 and $\tan\beta$, and for distinct seesaw scales. We set the R -matrix to $\mathbb{1}$ (see Eq. (4)), thus working in a conservative scenario where all flavour violation in the lepton sector arises from the U^{MNS} . In each panel, the blue lines denote $\text{BR}(\mu \rightarrow e\gamma)$ isolines: the former MEGA bound, 1.2×10^{-11} [70] (lower dashed line), the MEG current bound 5.7×10^{-13} [53] (solid line), as well as MEG's expected future sensitivity [71], 6×10^{-14} (upper dashed line). In addition, the region delimited by a thick dashed line is excluded by collider bounds [46–51], while the two solid pink lines correspond to having $m_h \in [123 \text{ GeV}, 128 \text{ GeV}]$, in agreement with LHC data [52]. Fig. 1 clearly manifests the effect

⁴The recent analysis of [69] suggests that charge and colour breaking minima constraints on the cMSSM parameter space, in particular in the regime of large $|A_0|$, can be more severe than previously thought. A detailed study of whether or not some of the points here considered are associated to an unstable desired EWSB minimum lies beyond the scope of our work. However, we expect that the large majority of points compatible with all bounds (including flavour) falls outside the instability regions identified in [69], where scenarios of large $|A_0|$ are typically associated to very large $M_{1/2}$ and/or even larger m_0 .

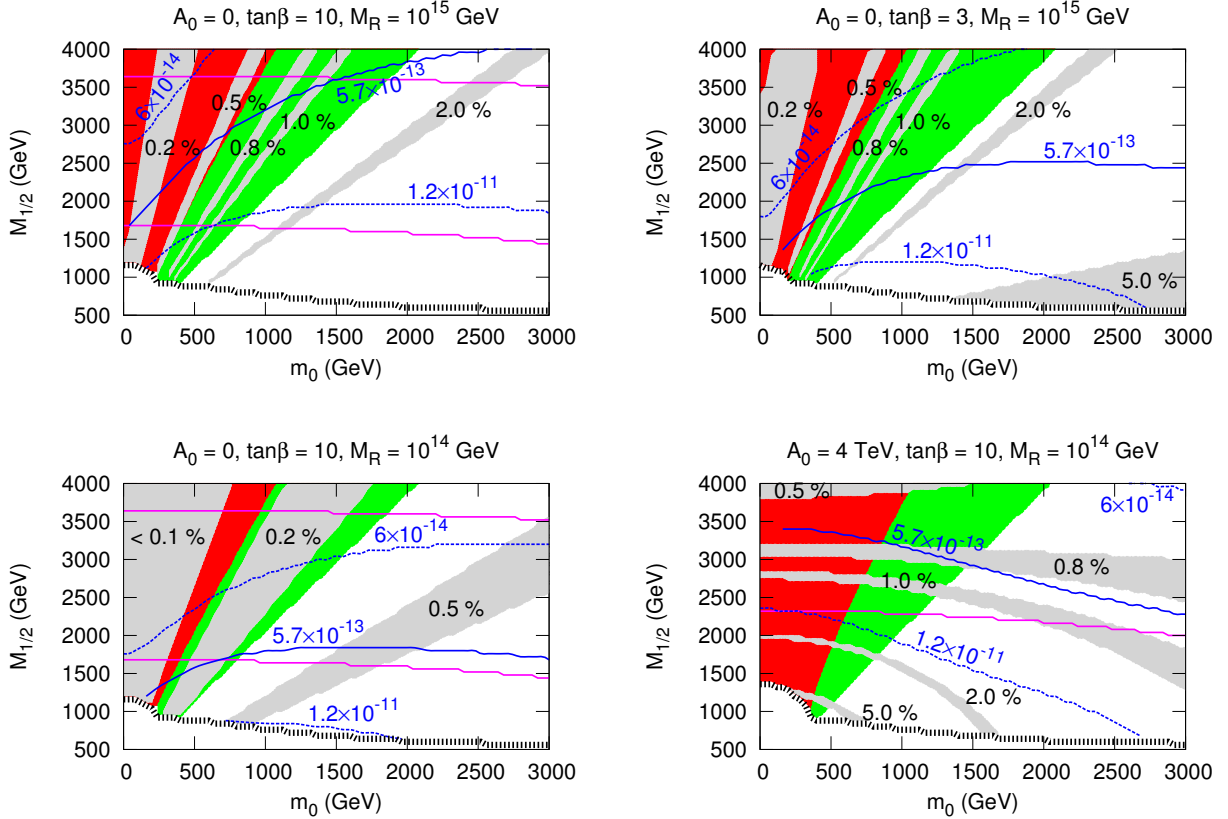


Figure 1: m_0 - $M_{1/2}$ plane for different choices of A_0 , $\tan\beta$ and seesaw scale (M_R), with different grey regions corresponding to distinct values of $\Delta m_{\tilde{e}_L, \tilde{\mu}_L}/m_{\tilde{e}}$ as indicated. We have taken a degenerate RH neutrino spectrum and set $R = \mathbb{1}$. The region below the thick (black) dashed curve does not pass the cuts applied on sparticle masses, while the red regions are excluded due to the presence of a charged LSP. Green regions correspond to $m_{\chi_{2,1}^0, \chi_{1,1}^\pm} > \langle m_{\tilde{e}_L}, m_{\tilde{\mu}_L} \rangle + 10$ GeV. Different blue curves denote $\text{BR}(\mu \rightarrow e\gamma)$ isolines, while the two solid pink lines enclose the region where $m_h \in [123 \text{ GeV}, 128 \text{ GeV}]$.

of the new $\text{BR}(\mu \rightarrow e\gamma)$ upper-limit, which in all cases amounts to dramatically reducing the previously allowed cMSSM SUSY-seesaw space. By lowering the seesaw scale (i.e., taking smaller values of M_R , and hence smaller Y^ν), larger regions of the m_0 - $M_{1/2}$ plane can survive. However, and as we proceed to discuss, this has a direct impact on the prospects for sizeable flavoured slepton mass splittings, as both observables stem from a unique source of LFV - the neutrino Yukawa couplings.

As can be seen in the top left panel of Fig. 1, the largest fractional mass splittings ($\Delta m_{\tilde{e}_L, \tilde{\mu}_L}/m_{\tilde{e}}$) correspond to regions with large m_0 . This can be understood from the fact that (flavour non-universal) RG-driven contributions to the soft masses of left-handed (LH) sleptons are proportional to $m_L^2 = m_{\nu_R}^2 = m_{H_2}^2 = m_0^2$ at M_{GUT} (cf. Eq. (5)). The predominant effect of a larger $M_{1/2}$ translates in the increase of the slepton soft-masses at the SUSY scale from radiative corrections involving EW gauginos. For the case of a comparatively large seesaw scale ($M_R \sim 10^{15}$ GeV), in association with large Yukawa couplings, $Y^\nu \sim \mathcal{O}(1)$, one could expect $\Delta m_{\tilde{e}_L, \tilde{\mu}_L}/m_{\tilde{e}} \approx 2\%$; however, these regions are associated to $\text{BR}(\mu \rightarrow e\gamma)$ already excluded. Complying with all

bounds (accelerator - including Higgs searches -, and low-energy), and further requiring a neutral LSP⁵, reduces the m_0 - $M_{1/2}$ plane to a small triangular region, corresponding to $m_0 \sim 1$ TeV, $M_{1/2} \sim 3.5$ TeV, where at most one can expect $\Delta m_{\tilde{\ell}}(\tilde{e}_L, \tilde{\mu}_L)/m_{\tilde{\ell}} \sim \mathcal{O}(1\%)$, typically for $m_{\tilde{\ell}_L} \approx 2.5$ TeV.

As mentioned before, lowering the seesaw scale reduces the amount of RG-induced cLFV. As manifest from the comparison of the left panels of Fig. 1, the new bound on $\text{BR}(\mu \rightarrow e\gamma)$ can now be accommodated in larger regions of the m_0 - $M_{1/2}$ plane, but slepton mass splittings also diminish, and one has $\Delta m_{\tilde{\ell}}(\tilde{e}_L, \tilde{\mu}_L)/m_{\tilde{\ell}} \lesssim 0.5\%$. Although this will be addressed in more detail in the following section, considering $R \neq 1$ would mostly lead to a displacement of the $\Delta m_{\tilde{\ell}}$ isosurfaces to larger values of m_0 , accompanied by distortions of the $\text{BR}(\mu \rightarrow e\gamma)$ isolines; a hierarchical RH spectrum (or fixed values of M_{R_3}) would in turn lead to a slight reduction of the associated $\text{BR}(\mu \rightarrow e\gamma)$.

The size (and global shape) of the different regions in the m_0 - $M_{1/2}$ plane also reflects the remaining mSUGRA parameters, A_0 and $\tan\beta$. The two lower panels of Fig. 1 reflect the impact of varying the trilinear couplings. For $|A_0| \gg m_0$, the A_0^2 contribution outweighs that of m_0^2 to the flavour non-universal radiative corrections (see Eq. (5)), so that in this case the mass splittings are approximately constant along the m_0 direction. In the regime of large $|A_0|$, one finds that the largest splittings compatible with flavour bounds are $\Delta m_{\tilde{\ell}}(\tilde{e}_L, \tilde{\mu}_L)/m_{\tilde{\ell}} \sim 0.8\%$, for sleptons heavier than several TeV. The effect of varying - in particular, lowering - $\tan\beta$ can be evaluated from the comparison of the two upper panels. Regimes of larger $\tan\beta$ lead to larger SUSY contributions to $\text{BR}(\mu \rightarrow e\gamma)$ [3,4], and compatibility with current bounds strongly constrains the size of the Yukawa couplings, thus reducing the maximal value of the slepton mass differences. Setting $\tan\beta = 3$ implies that in a strict cMSSM framework h is too light to be the SM-like Higgs. However, minimally relaxing the universal conditions (in particular concerning the third generation squark masses) to accommodate $m_h \sim 125$ GeV, without affecting considerably the observables being displayed, allows to infer that the low m_0 - $M_{1/2}$ regions that were excluded in the $\tan\beta = 10$ case by the upper-limit on $\mu \rightarrow e\gamma$ are now viable. In addition, they exhibit a small enhancement of the mass splittings due to an increase in the strength of Y^ν ($\propto 1/v_2$, cf. Eq.(4)). (Relaxed scenarios, which accommodate $m_h \sim 125$ GeV with light EW gauginos and sleptons, will be explored in Sec. 3.2.)

To summarise the crucial point of the first part of the analysis, Fig. 1 clearly reveals how the prospects for probing the cMSSM type-I seesaw have evolved in view of the recent experimental breakthroughs. While in a first analysis⁶ (pre-LHC) [35] one could have $\Delta m_{\tilde{\ell}}(\tilde{e}_L, \tilde{\mu}_L)/m_{\tilde{\ell}} \sim 5\%$ for $m_{\tilde{\ell}} \sim 500$ GeV, one is now confronted to a very different situation: at most one can expect $\Delta m_{\tilde{\ell}}(\tilde{e}_L, \tilde{\mu}_L)/m_{\tilde{\ell}} \sim 1\%$, and only in a somewhat fine-tuned region of the m_0 - $M_{1/2}$ plane, always in association with considerably heavy sleptons (~ 2.5 TeV). Whether or not the LHC will be able to reconstruct such tiny mass differences lies beyond the scope of the present analysis.

As mentioned in Section 2.2, at the LHC sleptons are preferably produced in $\tilde{q}_L \rightarrow \{\chi_2^0, \chi_1^\pm\} \rightarrow$

⁵In our analysis, and other than requiring that the LSP be neutral (typically the lightest neutralino), we do not impose dark matter constraints on the parameter space. For completeness, we notice that in general the relic density ($\Omega_{\text{DM}}h^2$) is always $\Omega_{\text{DM}}h^2 > 0.13$ [68], as points complying with recent bounds [72,73] lie below the direct search exclusion line. One can nevertheless consider non-standard cosmological models, where a deviation from standard Big-Bang cosmology allows to reduce the relic density [74], or a very small amount of R-parity violation that would render the LSP unstable.

⁶In a previous exploratory study [35], a regime of very small θ_{13} (prior to its experimental measurement) had been considered. For larger θ_{13} , the largest slepton mass splittings compatible with the same set of flavour bounds are smaller than those derived for small θ_{13} . In fact, in the case $R \approx 1$ and for $M_{R_3} \gg M_{R_{1,2}}$, smaller values of θ_{13} allow for a larger overall contribution to $\Delta m_{\tilde{\ell}}(\tilde{e}_L, \tilde{\mu}_L)/m_{\tilde{\ell}}$ (which can also proceed from $\tilde{\tau} - \tilde{\mu}$ mixing, less experimentally constrained).

$\tilde{\ell}_L$ decays (if kinematically allowed). In all panels of Fig. 1, green surfaces correspond to regions where $\tilde{\ell}_L$ can be produced from χ_2^0 decays, accompanied by the emission of a hard lepton. We will subsequently explore these regions in greater detail. In particular, and instead of considering a degenerate RH neutrino spectrum, we now consider a hierarchical one: we fix $M_{R_1} = 10^{10}$ GeV, $M_{R_2} = 10^{11}$ GeV with $M_{R_3} \in \{10^{12}, 10^{13}, 10^{14}, 10^{15}\}$ GeV. We again set $R = 1$. For each point we then perform a random scan in m_0 , $M_{1/2}$ and A_0 , which are chosen from the following wide ranges

$$m_0 \in [0, 3] \text{ TeV}, \quad M_{1/2} \in [0, 10] \text{ TeV}, \quad A_0 \in [-4, 4] \text{ TeV}. \quad (12)$$

The low-energy spectrum is subject to all the aforementioned cuts on sparticle (and lightest Higgs) masses. One further requires that the spectrum obeys $m_{\chi_2^0} > \langle m_{\tilde{e}_L}, m_{\tilde{\mu}_L} \rangle + 10$ GeV, and that χ_1^0 is the LSP. The results are collected in Fig. 2, where we display the slepton mass splittings versus the average slepton mass for the first two generations.

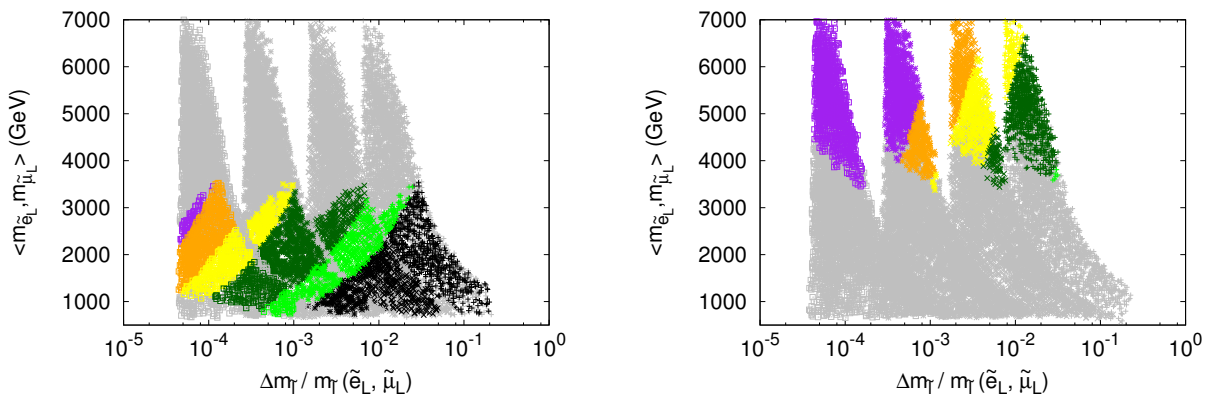


Figure 2: Slepton mass splittings versus the average slepton mass for the first two generations of mostly LH sleptons, in the cMSSM type-I seesaw. On the left we set $\tan \beta = 10$, while on the right $\tan \beta = 3$. We have taken $R = 1$ and a hierarchical RH neutrino spectrum with $M_{R_1} = 10^{10}$ GeV, $M_{R_2} = 10^{11}$ GeV and $M_{R_3} = \{10^{12}, 10^{13}, 10^{14}, 10^{15}\}$ GeV (corresponding to the four regions along the $\Delta m_{\tilde{\tau}}(\tilde{e}_L, \tilde{\mu}_L)/m_{\tilde{\tau}}$ axis). Grey points have m_h outside the preferred interval; purple, orange, yellow, dark-green, light-green and black regions correspond to $\text{BR}(\mu \rightarrow e\gamma)$ in the ranges $< 10^{-17}$, $[10^{-17}, 10^{-16}]$, $[10^{-16}, 10^{-15}]$, $[10^{-15}, 6 \times 10^{-14}]$, $[6 \times 10^{-14}, 5.7 \times 10^{-13}]$ and $> 5.7 \times 10^{-13}$, respectively.

Each of the panels of Fig. 2 comprises four “boomerang-shaped” regions, corresponding to the different choices of M_{R_3} (increasing from left to right). Within each individual region, the upwards (and left-most) part corresponds to regimes of small $|A_0|$ (compared to m_0 and $M_{1/2}$), while the right-most extremity is associated with larger $|A_0|$. As it is clear from the left panel (where $\tan \beta = 10$), any splittings $\gtrsim \mathcal{O}(1\%)$, compatible with current lepton flavour bounds, are associated to heavy sleptons, $m_{\tilde{\ell}} \sim 2$ TeV. In agreement to what could be expected from the discussion⁷ of Fig. 1, these large splittings can either occur for $M_{R_3} \approx 10^{15}$ GeV in the small $|A_0|$ regime or $M_{R_3} \approx 10^{14}$ GeV for large $|A_0|$; we find it worth emphasising that these sizeable splittings, which have an associated $\text{BR}(\mu \rightarrow e\gamma)$ in the range of MEG’s expected future sensitivity (light-green points) have a spectrum compatible with $m_h \sim 125$ GeV. It is nevertheless possible

⁷We notice that a degenerate RH neutrino spectrum was considered in the analysis of Fig. 1. For fixed values of M_{R_3} , a hierarchical RH spectrum leads to a slight reduction of the associated $\text{BR}(\mu \rightarrow e\gamma)$ – by around a factor 2 –, hence rendering viable part of the 1% band in the bottom-right panel of Fig. 1.

to have $\Delta m_{\tilde{\ell}(\tilde{e}_L, \tilde{\mu}_L)}/m_{\tilde{\ell}} \gtrsim \mathcal{O}(0.1\%)$, compatible with current flavour bounds and within MEG reach, for lighter sleptons.

For comparison, on the right panel of Fig. 2 we display an analogous study for $\tan\beta = 3$. As previously discussed, in such a regime, complying with m_h bounds requires very large values of m_0 and $M_{1/2}$ (in a strictly constrained MSSM framework), thus leading to extremely heavy sleptons (and gauginos), $m_{\tilde{\ell}_L} \gtrsim 3.5$ TeV. In turn, this precludes the possibility of observing cLFV transitions at MEG (essentially for any value of the mass splittings).

Figure 2 clearly suggests that scenarios with sizeable $\Delta m_{\tilde{\ell}(\tilde{e}_L, \tilde{\mu}_L)}/m_{\tilde{\ell}}$, in association to a slepton spectrum sufficiently light to be abundantly produced at the LHC, and with viable $\text{BR}(\mu \rightarrow e\gamma)$ are excluded, since in a constrained framework as the cMSSM, such regimes are not compatible with m_h . In the following, we consider the impact of relaxing the strict universality of the SUSY soft-breaking terms regarding slepton mass splittings.

3.2 Beyond mSUGRA-inspired universal conditions

We now consider a modified SUSY seesaw scheme in which one breaks strict universality for squark, slepton and Higgs soft-breaking terms at the GUT scale (but still preserving flavour universality). Moreover, soft breaking gluino and EW gaugino masses are also taken to be independent. This results in the following relations at M_{GUT} , yielding 7 free parameters in addition to $\tan\beta$ and $\text{sign}(\mu)$:

$$M_{1/2} \Rightarrow \begin{cases} M_1 = M_2 = M_{1/2}^{\text{EW}}, \\ M_3 = M_{1/2}^3, \end{cases} \quad m_0 \Rightarrow \begin{cases} m_{\tilde{L}} = m_{\tilde{e}} = m_{\tilde{\nu}_R} = m_{\tilde{e}}, \\ m_{\tilde{Q}} = m_{\tilde{u}} = m_{\tilde{d}} = m_{\tilde{q}}, \\ m_{\tilde{H}_1} = m_{\tilde{H}_2} = m_{\tilde{H}}^H, \end{cases} \quad A_0 \Rightarrow \begin{cases} A_0^l = A_0^\nu = A_0^\ell, \\ A_0^u = A_0^d = A_0^q. \end{cases} \quad (13)$$

For each of the two considered regimes for $\tan\beta$, we focus on the following specific choices for $M_{1/2}^3$, $m_{\tilde{q}}$ and A_0^q , which lead to $m_h \sim 125$ GeV (enhanced by radiative corrections involving heavy stops and/or large stop mixing),

$$\begin{aligned} \tan\beta = 10 : \quad & M_{1/2}^3 = 1.1 \text{ TeV}, \quad m_{\tilde{q}} = 1.5 \text{ TeV}, \quad A_0^q = -4 \text{ TeV}; \\ \tan\beta = 3 : \quad & M_{1/2}^3 = 4.7 \text{ TeV}, \quad m_{\tilde{q}} = 4.5 \text{ TeV}, \quad A_0^q = -15 \text{ TeV}; \end{aligned} \quad (14)$$

and, similar to what was done for Fig. 2, we conduct a random scan of the remaining parameters, which were varied in the following chosen intervals:

$$M_{1/2}^{\text{EW}} \in [0, 5] \text{ TeV}, \quad m_{\tilde{\ell}} \in [0, 3] \text{ TeV}, \quad m_0^H \in [0, 3] \text{ TeV}, \quad A_0^\ell \in [-5, 5] \text{ TeV}. \quad (15)$$

The results are collected in Fig. 3, the panels corresponding to $\tan\beta = 10$ (left) and $\tan\beta = 3$ (right). All points displayed are in agreement with LHC bounds on sparticle masses and on a SM-like Higgs mass. Moreover, the spectrum always fulfils $m_{\chi_2^0} > \langle m_{\tilde{e}_L}, m_{\tilde{\mu}_L} \rangle + 10$ GeV, with a χ_1^0 LSP.

As it is manifest from Fig. 3, the most interesting consequence of relaxing the strict cMSSM universality conditions concerns the possibility of having considerably lighter sleptons in association with sizeable mass splittings and still compatible with flavour bounds. This is particularly striking in the case of $\tan\beta = 3$ (right panel), where one can verify that sleptons as light as ~ 800 GeV (1.6 TeV) can be associated to $\mathcal{O}(0.1\%)$ ($\mathcal{O}(1\%)$) splittings, in agreement with all imposed constraints. For $\tan\beta = 10$ (displayed on the left panel), the impact of deviating from a strict cMSSM framework is somewhat less pronounced: one again finds that $\mathcal{O}(0.1\%)$ slepton

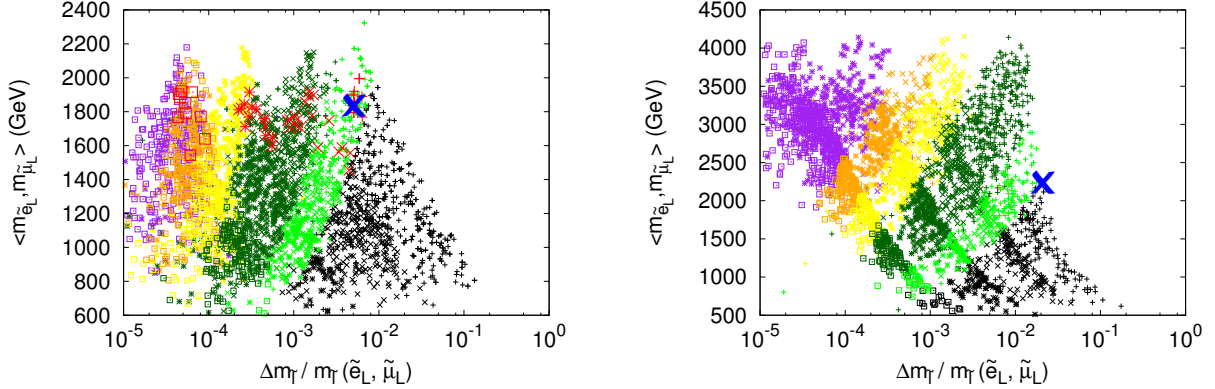


Figure 3: Mass splittings versus average mass for the first two generations of mostly LH sleptons, for the scenario of Eq. (13). The underlying scan is described in the text, with $\tan\beta = 10$ (3) in the left (right) panel. We have taken $R = \mathbb{1}$, and a hierarchical RH neutrino spectrum with $M_{R_1} = 10^{10}$ GeV, $M_{R_2} = 10^{11}$ GeV and $M_{R_3} = \{10^{12}, 10^{13}, 10^{14}, 10^{15}\}$ GeV. Colour code as in Fig. 2; in addition, we denote in red the points exhibiting a DM relic density $\Omega_{\text{DM}} h^2 < 0.13$. Superimposed blue “crosses” correspond to the sample points of Table 1.

mass splittings are attainable for $m_{\tilde{\ell}} \gtrsim 0.9$ TeV. Larger values of $\Delta m_{\tilde{\ell}}(\tilde{e}_L, \tilde{\mu}_L)/m_{\tilde{\ell}}$ remain difficult to obtain with the boundary conditions of Eq. (14).

A very interesting feature of this relaxed framework, especially for the $\tan\beta = 10$ case, is that the spectrum now allows for an efficient LSP density depletion (via $\chi_1^0 - \tilde{t}_1$ co-annihilation). This is highlighted by the red points in the left panel of Fig. 3.

Concerning the prospects of a potential future observation of a $\mu \rightarrow e\gamma$ decay at MEG, in the case of $\tan\beta = 10$, and for sleptons lighter than 1.2 TeV, $\Delta m_{\tilde{\ell}}(\tilde{e}_L, \tilde{\mu}_L)/m_{\tilde{\ell}} \gtrsim \mathcal{O}(0.1\%)$ are associated to $\text{BR}(\mu \rightarrow e\gamma)$ within MEG’s expected future sensitivity. For $\tan\beta = 3$, splittings $\gtrsim \mathcal{O}(1\%)$ ($\mathcal{O}(0.1\%)$), with sleptons lighter than ~ 2.7 TeV (1.3 TeV), would also yield $\text{BR}(\mu \rightarrow e\gamma)$ values within MEG reach.

As compared to Fig. 2, where one could still identify four independent “boomerang” shapes (especially for heavy sleptons), here only four small crests can be distinguished (again for the heavier slepton regimes). Due to having uncorrelated $m_0^{\tilde{q}}$ and m_0^H at the GUT scale, and having taken heavy stops (with large A_0^u), $m_{H_2}^2$ can now run to negative values above the seesaw scale, thus potentially cancelling the contribution of $m_{\tilde{\nu}_R}^2$, $m_{\tilde{L}}^2$ and $|A_0^u|^2$ to the flavour violating RG-induced effects (cf. Eq. (5)). Potential cancellations within the flavour-violating soft-breaking terms were pointed out in [56] for the case of non-universal Higgs masses (where possible negative values of $m_{H_2}^2$ at the GUT scale were considered). Finally, we notice that points in the left (right) panel have an average squark mass for the first two LH generations $m_{\tilde{q}_L} \sim 3$ (9) TeV. Although this formally means that all points displayed in Fig. 3 would have the $\tilde{q}_L \rightarrow \chi_2^0 \rightarrow \tilde{\ell}_L$ cascade open, in the general case the most likely slepton production mode remains via direct gaugino production (due to the very heavy squark spectrum).

In what follows we evaluate to which extent the correlations between low- and high-energy cLFV observables can still provide potential probes of a type-I SUSY seesaw, illustrating the results for two individual cases, singled out from the panels of Fig. 3, where they have been depicted using blue “crosses”.

Point A (left panel - $\tan\beta = 10$) exhibits the largest splittings for a light slepton spectrum,

and has $\Omega_{\text{DM}}h^2$ within the 1σ interval of Planck [72]. Point B (right panel - $\tan\beta = 3$) also corresponds to a choice illustrating the largest splittings still compatible with current flavour bounds. In Table 1 we display the SUSY soft breaking terms (in addition to the fixed input parameters of Eq. (14)), and a sample of the SUSY spectrum - corresponding to $M_{R_3} = 10^{15}$ GeV. Strictly for illustrative purposes, and using PROSPINO-2.1 [75], we also provide an estimation of the LH slepton production cross-sections for $\sqrt{s} = 14$ TeV, from the decay of directly produced neutral and charged winos (χ_2^0, χ_1^\pm), as well as from the decay chains of directly produced squarks and gluinos. (Notice that Point A is a concrete example of a case where slepton production via squark production is more favourable than via direct gaugino production.)

| | A | B |
|-----------------------|------|------|
| $M_{1/2}^{\text{EW}}$ | 2362 | 2821 |
| $m_0^{\tilde{\ell}}$ | 973 | 1365 |
| m_0^H | 173 | 2808 |
| A_0^ℓ | 3750 | 1651 |

| | A | B |
|--|-------|-------|
| $\langle m_{\tilde{e}_L}, m_{\tilde{\mu}_L} \rangle$ | 1835 | 2240 |
| $\frac{\Delta m_{\tilde{\ell}}}{m_{\tilde{\ell}}}(\tilde{e}_L, \tilde{\mu}_L)$ | 0.5% | 2.1% |
| $m_{\chi_2^0, \chi_1^\pm}$ | 1936 | 2349 |
| $m_{\chi_1^0}$ | 1043 | 1264 |
| $m_{\tilde{t}_1}$ | 1084 | 4825 |
| $\langle m_{\tilde{q}_L} \rangle$ | 2916 | 9059 |
| m_h | 125.4 | 125.3 |

| | A | B |
|---|----------------------|----------------------|
| $\sigma_{\tilde{\ell}}^{\text{prod}}(\chi_2^0, \chi_1^\pm)$ | 6.1×10^{-4} | 7.6×10^{-4} |
| $\sigma_{\tilde{\ell}}^{\text{prod}}(\chi_2^0 \text{ only})$ | 2.1×10^{-4} | 2.6×10^{-4} |
| $\sigma_{\tilde{\ell}}^{\text{prod}}(\tilde{q}_L; \text{via } \chi_2^0, \chi_1^\pm)$ | 1.9×10^{-2} | – |
| $\sigma_{\tilde{\ell}}^{\text{prod}}(\tilde{q}_L; \text{via } \chi_2^0 \text{ only})$ | 6.4×10^{-3} | – |

Table 1: Points A and B: SUSY soft breaking input parameters, sample of the SUSY spectrum and slepton mass splittings (in the case of $M_{R_3} = 10^{15}$ GeV), and LH slepton production cross-sections for $\sqrt{s} = 14$ TeV (masses in GeV and σ in fb).

Although the production cross-sections for these points suggest that observation of a significant number of events might be challenging, it is important to stress that a minor modification of the spectra (in particular, breaking the universality of the third generation of squarks) could easily lead to scenarios where as much as 300 events can be indeed achieved, for an integrated luminosity around 3000 fb^{-1} .

In Fig. 4 we display $\text{BR}(\mu \rightarrow e\gamma)$ as a function of $\Delta m_{\tilde{\ell}}(\tilde{e}_L, \tilde{\mu}_L)/m_{\tilde{\ell}}$ for points A (left panel) and B (right panel), considering different regimes of M_{R_3} (for fixed values of $M_{R_{1,2}}$). On the secondary y-axis we present the corresponding value of $\text{CR}(\mu - e, \text{Ti})$, estimated assuming the hypothesis of γ -penguin domination, valid for the scenarios here considered (see, for example [25, 59]), and which predicts $\text{CR}(\mu - e, \text{Ti}) \approx 5 \times 10^{-3} \text{ BR}(\mu \rightarrow e\gamma)$ [9]. A horizontal full (dashed) line corresponds to MEG's current bound (expected future sensitivity), while a cyan dashed line corresponds to PRISM/PRIME proposed sensitivity⁸, $\text{CR}(\mu - e, \text{Ti}) \sim 10^{-18}$ [78]. On the upper two plots, we

⁸Other proposals for high-sensitivity $\mu - e$ conversion searches (Aluminium nuclei) include Mu2e [76] and COMET [77].

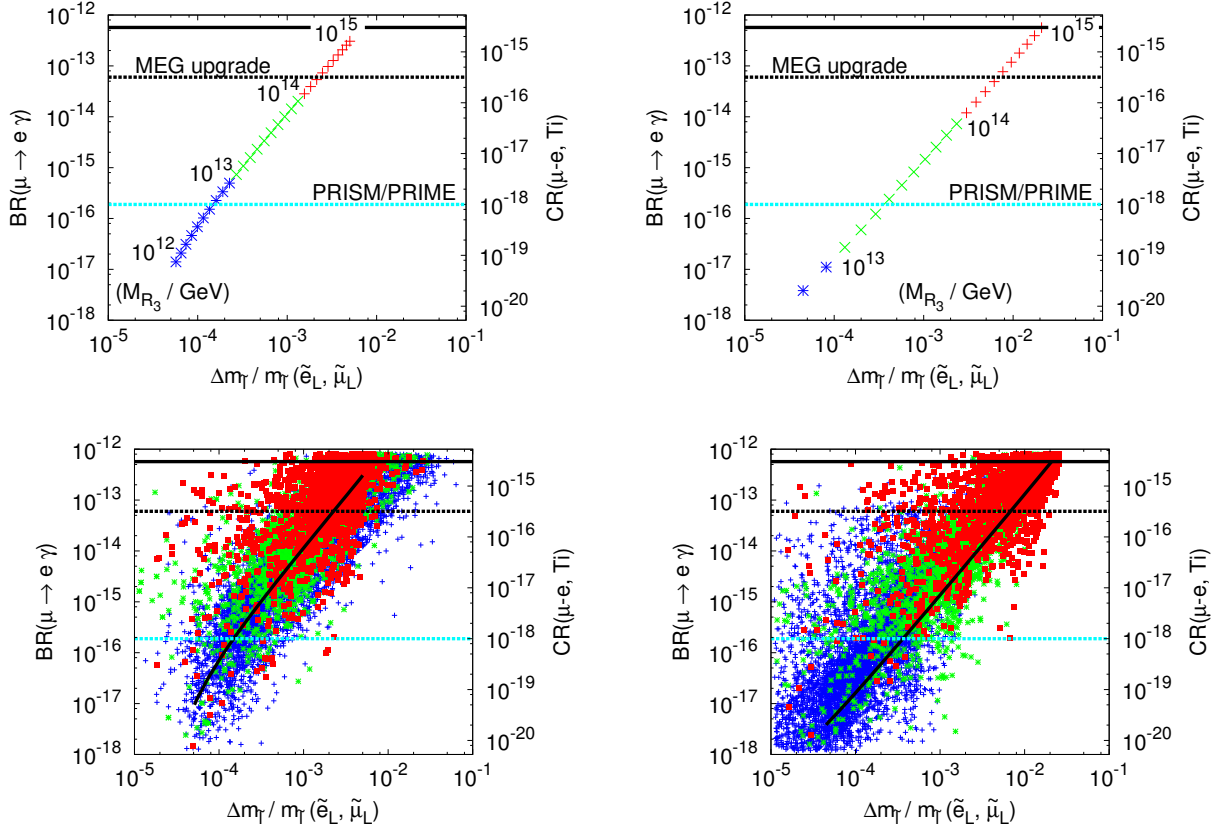


Figure 4: Mass splittings versus $\text{BR}(\mu \rightarrow e\gamma)$ for points A (left) and B (right) - see Table 1, displaying complementary information on $\text{CR}(\mu - e, \text{Ti})$ on the secondary y-axis. Full (dashed) horizontal lines denote current bounds (future sensitivities). We have taken a hierarchical RH neutrino spectrum with $M_{R_1} = 10^{10}$ GeV, $M_{R_2} = 10^{11}$ GeV. The colour scheme denotes different intervals of M_{R_3} : in the upper panels it is varied in the range $[10^{12}, 10^{15}]$ GeV, while in the lower panels we considered $10^{13,14,15}$ GeV (blue, green and red points, respectively). On the upper panels, we set $R = \mathbb{1}$, while in the lower ones the R -matrix was randomly varied in the intervals $|\theta_i| \lesssim \pi$ and $-\pi \lesssim \arg(\theta_i) \lesssim \pi$. The slanted full black lines on the lower panels correspond to the limit $R = \mathbb{1}$ depicted in the upper panels.

have again taken the conservative - yet simple - limit of $R = \mathbb{1}$. On the lower plots of Fig. 4, we consider the more general case where there are additional mixings involving the RH neutrinos, conducting a broad scan over the complex R -matrix angles, θ_i . This allows a global overview of the contributions to the different cLFV observables (albeit for fixed SUSY points).

The information contained in the different panels of Fig. 4 provides a comprehensive summary of the discussion we have conducted so far. Taking into account the additional degrees of freedom in the RH neutrino sector (encoded in the R -matrix complex angles) allows to have mass splittings as large as 5%, still in agreement with low-energy flavour bounds, and even for a comparatively low seesaw scale, $\mathcal{O}(10^{13}$ GeV), as made clear from the lower panels. Strong deviations from the simplistic $R = \mathbb{1}$ case may also point in the direction of particular flavour models, as recently explored in [41].

From the interplay of the different observables, and depending on the outcome of the distinct

low- and high-energy experiments, many conclusions can be drawn with respect to the viability of a type-I SUSY seesaw as the underlying mechanism.

Under the hypothesis that the slepton mass scale will have been determined (and the sparticle spectrum interpreted in terms of a high-scale SUSY model), a joint study of the low- and high-energy cLFV observables can offer important insight into the seesaw dynamics. Let us first consider the simple $R = \mathbb{1}$ case: for scenario A, any measurement of $\Delta m_{\tilde{\ell}}(\tilde{e}_L, \tilde{\mu}_L)/m_{\tilde{\ell}} \gtrsim 0.1\%$ would entail $\text{BR}(\mu \rightarrow e\gamma)$ within MEG reach (and vice-versa), further suggesting a seesaw scale of the order of 10^{14} GeV. For reconstructed SUSY models of lower $\tan\beta$, the result in the upper right panel would allow for similar conclusions: splittings of $\mathcal{O}(1\%)$ ($\mathcal{O}(0.1\%)$) should be accompanied by the observation of $\mu \rightarrow e\gamma$ decay at MEG ($\mu - e$ conversion at PRISM/PRIME), hinting towards a seesaw scale of the order of 5×10^{14} GeV (10^{14} GeV). Conversely, the isolated manifestation of either low- or high-scale cLFV, e.g. $\Delta m_{\tilde{\ell}}(\tilde{e}_L, \tilde{\mu}_L)/m_{\tilde{\ell}} \gtrsim \mathcal{O}(5\%)$ without any $\mu \rightarrow e\gamma$ or $\mu - e$ signal, would strongly suggest that sources of LFV, other than - or in addition to - the SUSY seesaw are present.

Analogous, but stronger conclusions can be drawn from the inspection of the scans corresponding to $R \neq \mathbb{1}$ case: although the clear dependence on the seesaw scale (present for $R = \mathbb{1}$) becomes diluted due to the additional contributions from the mixings involving RH neutrinos, the correlation between the observables still allows to indirectly test the SUSY seesaw. Again, any measurement $\Delta m_{\tilde{\ell}}(\tilde{e}_L, \tilde{\mu}_L)/m_{\tilde{\ell}} \gtrsim \mathcal{O}(1\%)$ must be accompanied by observation of $\mu \rightarrow e\gamma$ decay at MEG so to substantiate the SUSY seesaw hypothesis; on the other hand $\Delta m_{\tilde{\ell}}(\tilde{e}_L, \tilde{\mu}_L)/m_{\tilde{\ell}} \gtrsim \mathcal{O}(1\%)$ without any $\mu \rightarrow e\gamma$ or $\mu - e$ signal would strongly disfavour the underlying hypothesis.

4 Conclusions

In this study we have revisited the impact of a type-I SUSY seesaw concerning LFV following the recent MEG bound on $\text{BR}(\mu \rightarrow e\gamma)$, LHC data (discovery of a Higgs-like boson and negative SUSY searches), and the measurement of θ_{13} , updating the results obtained in [35]. The aim of our work was to discuss whether current cLFV results and SUSY searches still render viable the observation of slepton mass differences at the LHC, and if the interplay of the latter observables with low-energy cLFV bounds could still shed some light on the high-energy seesaw parameters. Our analysis was based in the hypothesis that all flavour violation in the lepton sector is due to the neutrino Yukawa couplings; we thus embed the type-I seesaw in constrained and semi-constrained SUSY breaking scenarios.

Due to the new $\text{BR}(\mu \rightarrow e\gamma)$ bound, in association with the measured “large” value of θ_{13} , we find that in general slepton mass splittings tend to be very small, unless the slepton spectra is considerably heavy. This implies that for the type-I SUSY seesaw the observation of cLFV at high-energies will be clearly much more challenging than the low-energy, high-intensity studies.

Regarding the embedding of the type-I seesaw into constrained SUSY models such as the cMSSM, we have verified that recent LHC data (in particular the measurement of m_h) precludes the possibility of simultaneously having $\text{BR}(\mu \rightarrow e\gamma)$ within MEG reach and sizeable slepton mass differences associated with a slepton spectrum sufficiently light to be produced.

On the other hand, relaxing the strict universality of SUSY soft-breaking terms allows to circumvent some of the strongest LHC bounds, especially on m_h , and opens the door to non-negligible slepton mass splittings (for a comparatively light slepton spectrum), with associated $\mu \rightarrow e\gamma$ rates (as well as $\text{CR}(\mu - e)$) within experimental reach. Although dependent on the SUSY regime (e.g., on $\tan\beta$), one can still find $\Delta m_{\tilde{\ell}}(\tilde{e}_L, \tilde{\mu}_L)/m_{\tilde{\ell}} \sim 0.1\% - 1\%$, for $m_{\tilde{\ell}}$ ranging from 800 GeV to 1.6 TeV.

We have studied in detail the impact of the different seesaw parameters for representative

points in SUSY space. The results of this comprehensive analysis were presented in Fig. 4. As we have shown, one can have mass splittings as large as 5%, still in agreement with low-energy flavour bounds, even for a comparatively low seesaw scale, $\mathcal{O}(10^{13}$ GeV). In these scenarios, one can still use the correlation of high- and low-energy cLFV observables to probe the SUSY seesaw, and we provided some illustrative examples of this interplay.

In summary, our analysis shows that in the case of semi-constrained (flavour universal) SUSY models, the reconstruction of the slepton mass scale and slepton mass splittings, in synergy with the measurement of low-energy cLFV observables, still remains a potential probe to test (strengthen or disfavour) the high-scale type-I SUSY seesaw.

Acknowledgements

We are indebted to A. Abada and J. C. Romão for many valuable exchanges and suggestions. The work of A. J. R. F. has been supported by *Fundação para a Ciência e a Tecnologia* through the fellowship SFRH/BD/64666/2009. A. J. R. F. acknowledges the financial support from the EU Network grant UNILHC PITN-GA-2009-237920 and from *Fundação para a Ciência e a Tecnologia* grants CFTP-FCT UNIT 777, CERN/FP/83503/2008 and PTDC/FIS/102120/2008. We also acknowledge partial support from the European Union FP7 ITN INVISIBLES (Marie Curie Actions, PITN-GA-2011-289442).

References

- [1] F. Borzumati and A. Masiero, *Phys. Rev. Lett.* **57** (1986) 961.
- [2] P. Minkowski, *Phys. Lett. B* **67** (1977) 421; M. Gell-Mann, P. Ramond and R. Slansky, in *Complex Spinors and Unified Theories* eds. P. Van. Nieuwenhuizen and D. Z. Freedman, *Supergravity* (North-Holland, Amsterdam, 1979), p.315 [Print-80-0576 (CERN)]; T. Yanagida, in *Proceedings of the Workshop on the Unified Theory and the Baryon Number in the Universe*, eds. O. Sawada and A. Sugamoto (KEK, Tsukuba, 1979), p.95; S. L. Glashow, in *Quarks and Leptons*, eds. M. Lévy *et al.* (Plenum Press, New York, 1980), p.687; R. N. Mohapatra and G. Senjanović, *Phys. Rev. Lett.* **44** (1980) 912.
- [3] J. Hisano, T. Moroi, K. Tobe and M. Yamaguchi, *Phys. Rev. D* **53** (1996) 2442 [hep-ph/9510309].
- [4] J. Hisano, T. Moroi, K. Tobe, M. Yamaguchi and T. Yanagida, *Phys. Lett. B* **357** (1995) 579 [hep-ph/9501407].
- [5] J. Hisano and D. Nomura, *Phys. Rev. D* **59** (1999) 116005 [arXiv:hep-ph/9810479].
- [6] W. Buchmuller, D. Delepine and F. Vissani, *Phys. Lett. B* **459** (1999) 171 [arXiv:hep-ph/9904219].
- [7] Y. Kuno and Y. Okada, *Rev. Mod. Phys.* **73** (2001) 151 [arXiv:hep-ph/9909265].
- [8] J. R. Ellis, M. E. Gomez, G. K. Leontaris, S. Lola and D. V. Nanopoulos, *Eur. Phys. J. C* **14** (2000) 319 [hep-ph/9911459].
- [9] J. Hisano and K. Tobe, *Phys. Lett. B* **510** (2001) 197 [hep-ph/0102315].
- [10] J. A. Casas and A. Ibarra, *Nucl. Phys. B* **618** (2001) 171 [hep-ph/0103065].

- [11] S. Lavignac, I. Masina and C. A. Savoy, *Phys. Lett. B* **520** (2001) 269 [arXiv:hep-ph/0106245].
- [12] X. J. Bi and Y. B. Dai, *Phys. Rev. D* **66** (2002) 076006 [arXiv:hep-ph/0112077].
- [13] J. R. Ellis, J. Hisano, M. Raidal and Y. Shimizu, *Phys. Rev. D* **66** (2002) 115013 [hep-ph/0206110].
- [14] F. Deppisch, H. Pas, A. Redelbach, R. Ruckl and Y. Shimizu, *Eur. Phys. J. C* **28** (2003) 365 [arXiv:hep-ph/0206122].
- [15] T. Fukuyama, T. Kikuchi and N. Okada, *Phys. Rev. D* **68** (2003) 033012 [arXiv:hep-ph/0304190].
- [16] A. Brignole and A. Rossi, *Nucl. Phys. B* **701** (2004) 3 [arXiv:hep-ph/0404211].
- [17] A. Masiero, S. K. Vempati and O. Vives, *New J. Phys.* **6** (2004) 202 [arXiv:hep-ph/0407325].
- [18] T. Fukuyama, A. Ilakovac and T. Kikuchi, *Eur. Phys. J. C* **56** (2008) 125 [arXiv:hep-ph/0506295].
- [19] S. T. Petcov, W. Rodejohann, T. Shindou and Y. Takahashi, *Nucl. Phys. B* **739** (2006) 208 [arXiv:hep-ph/0510404].
- [20] E. Arganda and M. J. Herrero, *Phys. Rev. D* **73** (2006) 055003 [hep-ph/0510405].
- [21] F. Deppisch, H. Pas, A. Redelbach and R. Ruckl, *Phys. Rev. D* **73** (2006) 033004 [hep-ph/0511062].
- [22] C. E. Yaguna, *Int. J. Mod. Phys. A* **21** (2006) 1283 [arXiv:hep-ph/0502014].
- [23] L. Calibbi, A. Faccia, A. Masiero and S. K. Vempati, *Phys. Rev. D* **74** (2006) 116002 [arXiv:hep-ph/0605139].
- [24] S. Antusch, E. Arganda, M. J. Herrero and A. M. Teixeira, *JHEP* **0611** (2006) 090 [hep-ph/0607263].
- [25] E. Arganda, M. J. Herrero and A. M. Teixeira, *JHEP* **0710** (2007) 104 [arXiv:0707.2955 [hep-ph]].
- [26] E. Arganda, M. J. Herrero and J. Portoles, *JHEP* **0806** (2008) 079 [arXiv:0803.2039 [hep-ph]].
- [27] N. Arkani-Hamed, H. Cheng, J. L. Feng and L. J. Hall, *Phys. Rev. Lett.* **77** (1996) 1937 [arXiv:hep-ph/9603431].
- [28] I. Hinchliffe and F. E. Paige, *Phys. Rev. D* **63** (2001) 115006 [arXiv:hep-ph/0010086].
- [29] D. F. Carvalho, J. R. Ellis, M. E. Gomez, S. Lola and J. C. Romao, *Phys. Lett. B* **618** (2005) 162 [arXiv:hep-ph/0206148].
- [30] M. R. Buckley and H. Murayama, *Phys. Rev. Lett.* **97** (2006) 231801 [arXiv:hep-ph/0606088].
- [31] M. Hirsch, J. W. F. Valle, W. Porod, J. C. Romao and A. Villanova del Moral, *Phys. Rev. D* **78** (2008) 013006 [arXiv:0804.4072].
- [32] E. Carquin, J. Ellis, M. E. Gomez, S. Lola and J. Rodriguez-Quintero, *JHEP* **0905** (2009) 026 [arXiv:0812.4243].

- [33] J. N. Esteves, J. C. Romao, A. Villanova del Moral, M. Hirsch, J. W. F. Valle and W. Porod, *JHEP* **0905** (2009) 003 [arXiv:0903.1408 [hep-ph]].
- [34] A. J. Buras, L. Calibbi and P. Paradisi, *JHEP* **1009** (2010) 042 [arXiv:0912.1309].
- [35] A. Abada, A. J. R. Figueiredo, J. C. Romao and A. M. Teixeira, *JHEP* **1010** (2010) 104 [arXiv:1007.4833 [hep-ph]].
- [36] A. Abada, A. J. R. Figueiredo, J. C. Romao and A. M. Teixeira, *JHEP* **1108** (2011) 099 [arXiv:1104.3962 [hep-ph]].
- [37] L. Calibbi, R. N. Hodgkinson, J. Jones Perez, A. Masiero and O. Vives, *Eur. Phys. J. C* **72** (2012) 1863 [arXiv:1111.0176 [hep-ph]].
- [38] I. Galon and Y. Shadmi, *Phys. Rev. D* **85** (2012) 015010 [arXiv:1108.2220 [hep-ph]].
- [39] C. Arbelaez, M. Hirsch and L. Reichert, *JHEP* **1202** (2012) 112 [arXiv:1112.4771 [hep-ph]].
- [40] A. Abada, A. J. R. Figueiredo, J. C. Romao and A. M. Teixeira, *JHEP* **1208** (2012) 138 [arXiv:1206.2306 [hep-ph]].
- [41] M. Cannoni, J. Ellis, M. E. Gomez and S. Lola, *Phys. Rev. D* **88** (2013) 075005 [arXiv:1301.6002 [hep-ph]].
- [42] K. Abe *et al.* [T2K Collaboration], *Phys. Rev. Lett.* **107** (2011) 041801 [arXiv:1106.2822 [hep-ex]].
- [43] Y. Abe *et al.* [DOUBLE-CHOOZ Collaboration], *Phys. Rev. Lett.* **108** (2012) 131801 [arXiv:1112.6353 [hep-ex]].
- [44] J. K. Ahn *et al.* [RENO Collaboration], *Phys. Rev. Lett.* **108** (2012) 191802 [arXiv:1204.0626 [hep-ex]].
- [45] F. P. An *et al.* [Daya Bay Collaboration], *Chin. Phys. C* **37** (2013) 011001 [arXiv:1210.6327 [hep-ex]].
- [46] G. Aad *et al.* [ATLAS Collaboration], “Search for squarks and gluinos with the ATLAS detector in final states with jets and missing transverse momentum and 20.3 fb⁻¹ of $\sqrt{s} = 8$ TeV proton-proton collision data,” ATLAS-CONF-2013-047.
- [47] S. Chatrchyan *et al.* [CMS Collaboration], “Search for top-squark pair production in the single lepton final state in pp collisions at 8 TeV,” CMS-PAS-SUS-13-011; G. Aad *et al.* [ATLAS Collaboration], “Search for direct production of the top squark in the all-hadronic $t\bar{t}$ + e miss final state in 21 fb-1 of p-p collisions at $\sqrt{s}=8$ TeV with the ATLAS detector,” ATLAS-CONF-2013-024; G. Aad *et al.* [ATLAS Collaboration], “Search for direct third generation squark pair production in final states with missing transverse momentum and two b -jets in $\sqrt{s} = 8$ TeV pp collisions with the ATLAS detector,” ATLAS-CONF-2013-053; G. Aad *et al.* [ATLAS Collaboration], “Search for strongly produced superpartners in final states with two same sign leptons with the ATLAS detector using 21 fb-1 of proton-proton collisions at $\sqrt{s}=8$ TeV,” ATLAS-CONF-2013-007.
- [48] S. Chatrchyan *et al.* [CMS Collaboration], “Search for direct EWK production of SUSY particles in multilepton modes with 8TeV data,” CMS-PAS-SUS-12-022.

- [49] G. Aad *et al.* [ATLAS Collaboration], “Search for electroweak production of supersymmetric particles in final states with at least two hadronically decaying taus and missing transverse momentum with the ATLAS detector in proton-proton collisions at $\sqrt{s} = 8$ TeV,” ATLAS-CONF-2013-028.
- [50] G. Aad *et al.* [ATLAS Collaboration], “Search for direct-slepton and direct-chargino production in final states with two opposite-sign leptons, missing transverse momentum and no jets in 20/fb of pp collisions at $\sqrt{s} = 8$ TeV with the ATLAS detector,” ATLAS-CONF-2013-049.
- [51] S. Chatrchyan *et al.* [CMS Collaboration], JHEP **07** (2013) 122 [arXiv:1305.0491 [hep-ex]].
- [52] G. Aad *et al.* [ATLAS Collaboration], Phys. Lett. B **716** (2012) 1 [arXiv:1207.7214 [hep-ex]]; G. Aad *et al.* [ATLAS Collaboration], “Combined measurements of the mass and signal strength of the Higgs-like boson with the ATLAS detector using up to 25 fb⁻¹ of proton-proton collision data,” ATLAS-CONF-2013-014; G. Aad *et al.* [ATLAS Collaboration], “Combined coupling measurements of the Higgs-like boson with the ATLAS detector using up to 25 fb⁻¹ of proton-proton collision data,” ATLAS-CONF-2013-034; S. Chatrchyan *et al.* [CMS Collaboration], JHEP **06** (2013) 081 [arXiv:1303.4571 [hep-ex]].
- [53] J. Adam *et al.* [MEG Collaboration], Phys. Rev. Lett. **110** (2013) 201801 [arXiv:1303.0754 [hep-ex]].
- [54] R.-D. Heuer, “News from CERN, LHC Status and Strategy for Linear Colliders,” arXiv:1202.5860 [physics.acc-ph].
- [55] A. Barr, K. Boone, A. Canepa, M. Crispin, M. D’Onofrio, C. Young, G. Polesello and G. Redlinger, “Searches for Supersymmetry at the high luminosity LHC with the ATLAS Detector,” ATL-PHYS-PUB-2013-002.
- [56] L. Calibbi, D. Chowdhury, A. Masiero, K. M. Patel and S. K. Vempati, JHEP **1211** (2012) 040 [arXiv:1207.7227].
- [57] Y. Grossman and H. E. Haber, Phys. Rev. Lett. **78** (1997) 3438 [hep-ph/9702421].
- [58] M. Raidal *et al.*, Eur. Phys. J. C **57** (2008) 13 [arXiv:0801.1826 [hep-ph]] and references therein.
- [59] M. Arana-Catania, S. Heinemeyer and M. J. Herrero, Phys. Rev. D **88** (2013) 015026 [arXiv:1304.2783 [hep-ph]].
- [60] B. Aubert *et al.* [BaBar Collaboration], Phys. Rev. Lett. **104** (2010) 021802 [arXiv:0908.2381 [hep-ex]].
- [61] I. Hinchliffe, F. E. Paige, M. D. Shapiro, J. Soderqvist and W. Yao, Phys. Rev. D **55** (1997) 5520 [hep-ph/9610544].
- [62] B. C. Allanach, C. G. Lester, M. A. Parker and B. R. Webber, JHEP **0009** (2000) 004 [hep-ph/0007009].
- [63] H. Bachacou, I. Hinchliffe and F. E. Paige, Phys. Rev. D **62** (2000) 015009 [hep-ph/9907518].
- [64] M. C. Gonzalez-Garcia, M. Maltoni, J. Salvado and T. Schwetz, JHEP **1212** (2012) 123 [arXiv:1209.3023 [hep-ph]].

- [65] W. Porod, *Comput. Phys. Commun.* **153** (2003) 275 [hep-ph/0301101]. W. Porod and F. Staub, *Comput. Phys. Commun.* **183** (2012) 2458 [arXiv:1104.1573 [hep-ph]].
- [66] P. Bechtle, O. Brein, S. Heinemeyer, O. Stal, T. Stefaniak, G. Weiglein and K. Williams, *PoS CHARGED 2012* (2012) 024 [arXiv:1301.2345 [hep-ph]].
- [67] J. Beringer *et al.* [Particle Data Group Collaboration], *Phys. Rev. D* **86** (2012) 010001.
- [68] G. Belanger, F. Boudjema, A. Pukhov and A. Semenov, “micrOMEGAs3.1 : a program for calculating dark matter observables,” arXiv:1305.0237 [hep-ph].
- [69] J. E. Camargo-Molina, B. O’Leary, W. Porod and F. Staub, “Stability of the CMSSM against sfermion VEVs,” arXiv:1309.7212 [hep-ph].
- [70] M. L. Brooks *et al.* [MEGA Collaboration], *Phys. Rev. Lett.* **83** (1999) 1521 [hep-ex/9905013].
- [71] A. M. Baldini *et al.*, “MEG Upgrade Proposal,” arXiv:1301.7225 [physics.ins-det].
- [72] P. A. R. Ade *et al.* [Planck Collaboration], “Planck 2013 results. XV. CMB power spectra and likelihood,” arXiv:1303.5075 [astro-ph.CO].
- [73] G. Hinshaw *et al.* [WMAP Collaboration], *Astrophys. J. Suppl.* **208** (2013) 19 arXiv:1212.5226 [astro-ph.CO].
- [74] G. Gelmini, P. Gondolo, A. Soldatenko and C. E. Yaguna, *Phys. Rev. D* **74** (2006) 083514 [hep-ph/0605016]. G. B. Gelmini and P. Gondolo, *Phys. Rev. D* **74** (2006) 023510 [hep-ph/0602230].
- [75] W. Beenakker, R. Hopker, M. Spira and P. M. Zerwas, *Nucl. Phys. B* **492** (1997) 51 [hep-ph/9610490]; W. Beenakker, M. Klasen, M. Kramer, T. Plehn, M. Spira and P. M. Zerwas, *Phys. Rev. Lett.* **83** (1999) 3780 [Erratum-ibid. **100** (2008) 029901] [hep-ph/9906298], *Phys. Rev. Lett.* **83** (1999) 3780 [Erratum-ibid. **100** (2008) 029901] [hep-ph/9906298].
- [76] A. Gaponenko [mu2e Collaboration], “The Mu2e Experiment: A New High-Sensitivity Muon to Electron Conversion Search at Fermilab,” FERMILAB-CONF-12-490-PPD.
- [77] Y. Kuno [COMET Collaboration], *PTEP* **2013** (2013) 022C01.
- [78] R. J. Barlow, *Nucl. Phys. Proc. Suppl.* **218** (2011) 44.